An efficient system for selectively altering genetic information within mRNAs

Maria Fernanda Montiel-González[1,†], Isabel C. Vallecillo-Viejo[1,2,†] and Joshua J. C. Rosenthal[1,3,*]

[1]Institute of Neurobiology, University of Puerto Rico Medical Sciences Campus, San Juan, PR 00901, USA,
[2]Department of Pharmacology, University of Puerto Rico Medical Sciences Campus, San Juan, PR 00936, USA and
[3]The Marine Biological Laboratory, University of Chicago, Woods Hole, MA 02543, USA

ABSTRACT

Site-directed RNA editing (SDRE) is a strategy to precisely alter genetic information within mRNAs. By linking the catalytic domain of the RNA editing enzyme ADAR to an antisense guide RNA, specific adenosines can be converted to inosines, biological mimics for guanosine. Previously, we showed that a genetically encoded iteration of SDRE could target adenosines expressed in human cells, but not efficiently. Here we developed a reporter assay to quantify editing, and used it to improve our strategy. By enhancing the linkage between ADAR's catalytic domain and the guide RNA, and by introducing a mutation in the catalytic domain, the efficiency of converting a UAG premature termination codon (PTC) to tryptophan (UGG) was improved from ∼11 % to ∼70 %. Other PTCs were edited, but less efficiently. Numerous off-target edits were identified in the targeted mRNA, but not in randomly selected endogenous messages. Off-target edits could be eliminated by reducing the amount of guide RNA with a reduction in on-target editing. The catalytic rate of SDRE was compared with those for human ADARs on various substrates and found to be within an order of magnitude of most. These data underscore the promise of site-directed RNA editing as a therapeutic or experimental tool.

INTRODUCTION

Many of the most powerful tools in modern biology and medicine enable the manipulation of genetic information. In biology, they allow the researcher to characterize the function of gene products and the roles that they play in larger networks. In medicine, they regulate gene expression and hold tremendous promise for the correction of genetic mutations and the fine-tuning of protein function. To date, most approaches focus on knocking out genes, or manipulating their expression levels using processes like RNA interference (1,2). More recently, strategies for genome editing have unlocked more subtle manipulations, allowing researchers to alter protein function through codon-level engineering (3). A common theme among all strategies is that they are based on naturally occurring enzymatic systems. Although most focus on DNA, in theory, genetic information can be manipulated at any point before being realized as a protein.

RNA editing by adenosine deamination is a natural process of site-directed mutagenesis used by all true metazoans. It is catalyzed by the ADAR (Adenosine Deaminase that Acts on RNA) family of enzymes, which convert adenosine (A) to inosine (I) through a simple hydrolytic deamination (4–8). During translation and other biological processes, I is interpreted as guanosine (G; 9); thus the introduction of I within codons can recode them. Although A's make up about a quarter of all bases in RNAs, ADARs have the remarkable capacity to select specific ones for deamination. ADARs are modular, being composed of double stranded RNA binding motifs (dsRBMs) followed by a catalytic domain, often referred to as the deaminase domain (DD; 6,8). To edit a specific A, the dsRBMs bind to imperfect double-stranded structures and position the DD next to the target A (10). Obviously, RNA editing could be a useful tool if it could be directed towards a chosen A. The endogenous targeting mechanism, however, presents a barrier because it requires structures in *cis*, and these would be difficult to create.

Two similar strategies have been developed to target ADARs (11–16). For both, the dsRBMs have been removed and replaced with an antisense RNA guide. Because the RNA guide can be designed to bind to any primary RNA sequence, targeting is simple, depending only on Watson and Crick base-pairing. The RNA guide also plays the added

---

role of providing the double-stranded structure required by the DD (10). The two strategies differ by the way the DD is linked to the RNA guide. Our group has used the λN peptide-boxB hairpin RNA interaction, a small RNA binding protein and its target (11,17–19). The λN peptide is fused to the N-terminus of the DD from human ADAR2 (λN-DD), and the boxB hairpin is fused to the RNA guide. Although the interaction is not covalent, it is of nanomolar affinity and the components are small, making it less likely that they will interfere with the activity of the DD (11). This strategy allows both the guide and the editing enzyme to be fully genetically encoded, an important consideration for future delivery schemes. It also permits the relative proportion of the guide RNA and DD to be adjusted. Another group has used a SNAP-tag to join the DD to the RNA guide (12–16). This approach has the advantage of using a covalent interaction, and it also allows the addition of modified nucleotides to the guide RNA to provide added stability and specificity. Although the SNAP-tag containing DD is genetically encodable, the guide RNA must be delivered in its final form because it needs to be synthesized with a benzylguanine derivative, the substrate for the SNAP-tag. Both strategies have shown good success and hold much promise in developing the future potential of SDRE.

Although SDRE has been effectively employed to edit specific A's, there are hurdles to overcome. Thus far it has been effective *in vitro*, in *Xenopus* oocytes, in human cells, and, for the first time, in a simple animal model (annelid; 11–16); However, the extent of editing has not been rigorously quantified in cells. Using the λN-boxB system, editing was highly efficient when purified components were used *in vitro*. Using a semi-genetically encoded system in *Xenopus* oocytes, editing was moderately efficient. A fully genetically encoded version in human cells edited at low efficiency. Another issue is that the DD of ADAR prefers A's surrounded by specific neighbors (20,21), making some A's easier to target than others. Finally, the extent of off-target editing has not been rigorously evaluated. In this work, we systematically improved the λN-boxB system so that it can efficiently edit A's in a variety of neighboring contexts within human cells. In addition, we quantified off-target editing, determined how to reduce it, and compared the reaction kinetics of λN-DD with WT ADAR.

MATERIALS AND METHODS

Molecular biology

Because our experiments required three elements, we describe the production of the RNA guides, the various λN-DDs, and the target mRNAs separately. RNA guides were used for *in vitro* and *in cellula* experiments, and in each case they were made differently. For *in vitro* RNA guides, double-stranded oligo templates were synthesized with a T7 promoter and RNA was transcribed directly from them using the mScript™ Standard mRNA Production System (CellScript, Madison, WI, USA). For *in cellula* experiments, double stranded DNA oligonucleotides encoding the guide were cloned into the BLOCK-iT™ U6 RNAi Entry Vector (Invitrogen, Carlsbad, CA, USA).

The original λN-DD construct has been described previously (11). Sequence encoding additional λNs, and a short linker to connect them, was added to the N-terminus by synthesizing corresponding gene blocks and cloning them into the original vector by the Gibson Assembly Method (Gibson Assembly® Master Mix Kit, New England Biolabs, Ipswich, MA). A single λN-linker unit was MNARTRRRERRAEKQAQWKAAN–GGGGSGGGGSGGGGS. The same approach was used to introduce the R7K, R8K, and R11K mutants into both λN-DD and 4λN-DD (see Supporting Table S1). The E488Q mutation was added to the DD using the Quikchange Lightning Site-directed Mutagenesis kit (Agilent Technologies, Santa Clara, CA). The no-λN construct was made from λN-DD using inverse PCR (see Supporting Table S1).

There were two target mRNAs for this study: CFTR and mCherry-eGFP. CFTR, which was kindly provided by Dr. David Gadsby from the Rockefeller University, New York, has been described previously (11). CFTR RNA was used as a generic *in vitro* target, and was used only for the purpose of optimizing RNA guides. CFTR RNA was transcribed using the T7 RNA polymerase and the same RNA production kit above. The mCherry-eGFP and the mCherry-eGFP W58X constructs were synthesized by Genewiz, Inc. (South Plainfield, NJ) and subcloned via the XhoI and BamHI restriction sites into pcDNA 3.1(−) (Invitrogen, Carlsbad, CA, USA). This construct was used for RNA synthesis using the T7 RNA polymerase and the same RNA production kit and was also used for transfection into cells. For experiments involving PTCs in different neighboring contexts, the Quikchange Lightning Site-Directed Mutagenesis Kit was used to introduce substitutions at W58 and Y67 so that a target adenosine was located within every possible PTC context. All DNA oligonucleotides and gene blocks were purchased from Integrated DNA Technologies, Inc. (Coralville, IA, USA). The sequences of all constructs were verified by Sanger DNA sequencing and are given in Supporting Table S2 and Supporting Sequences S1.

λN-DD production in *Pichia pastoris*

Purification of all versions of λN-DD from *Pichia pastoris* has been described previously (11,22–24) and the protocol remains unchanged. In brief, N-terminal FLAG and C-terminal HIS-tagged constructs were cloned into the SpeI site of pPICZA-FLIS6 and transformed into *Pichia pastoris* strain SMD116H. Colonies able to grow on YPDS agar plates (1 % yeast extract, 2 % peptone, 2 % glucose, 2 % agar and 1 M sorbitol) supplemented with 1500 μg/ml Zeocin® were selected for expression. For protein purification, 500 ml cultures were grown in BMGY (1% yeast extract, 2 % peptone, 100 mM potassium phosphate, pH 6.0, 1.34 % yeast mannitol broth, 4×10^{-5} % biotin, and 1% glycerol) until OD600 reached 3 and then induced by changing the media to BMMY (same as BMGY but with 0.5 % methanol instead of 1 % glycerol). Cells were disrupted using a French Pressure Cell and proteins were purified by sequential Ni^{2+}-nitriloacetic acid column (QIAGEN, Hilden, Germany) and α-FLAG M2 column (Sigma-Aldrich, St Louis, MO, USA) purifications. Examples of purified proteins for all constructs are given in Supporting Figure S1.

In vitro editing assays

In vitro editing assays on CFTR RNA were performed as described previously (11). All *in vitro* editing assays on mCherry-eGFP W58X RNA were performed as described below. Prior to the editing assay, the RNA guide was annealed to the target RNA using a temperature ramp from 65 to 25°C, decreasing 1°C every 15 s. For reaction rate experiments, editing assays were performed under single turnover conditions at either 15°C or 35°C and time points were taken at 0, 1, 2, 5, 10, 20, 40, 60, 120 and 240 min. All assays contained 20 fmol target RNA, 200 fmol guide RNA (either 1BoxB or 2BoxB Guide), 360 fmol editase, 5 mM DTT, 5 nM PMSF, 0.5 μg/ul tRNA and 1 U/ul murine RNase inhibitor, all in Q200 [50 mM Tris-glutamate pH 7.0, 200 mM potassium glutamate, and 20 % (w/v) glycerol]. For extrapolating reported reaction rates from other ADARs to 15°C, a Q_{10} of 3.2 was used [$Q_{10} = (R_2/R_1)^{10/(T2-T1)}$]. This value was based on measurements of λN-DD editing of mCherry-eGFP W58X at 15°C and 35°C.

Quantification of editing efficiency *in vitro*

Quantification of editing efficiency was performed by RT-PCR and direct sequencing of PCR products as previously reported (11). Quantification was based on C/T peak heights of the anti-sense strand because it is more accurate than estimates based on the A/G peak heights of the sense strand (21,25). However, it should be noted that for display in the figures and supporting material all electropherograms have been reverse complemented for the sake of clarity of presentation. To estimate *in vitro* editing rates for all reactions except 2boxB λN-DD, reaction kinetics were fit to an equation of the form $E = E_{max} (1 - e^{-kt})$, where E = inosines produced, E_{max} = maximum inosine production, k = rate constant (min^{-1}) and t = time in minutes. Data for 2boxB λN-DD required a double exponential of the form $E = E_{max} + E_1 * e^{-k1t} + E_2 * e^{-k2t}$, where E_1 and E_2 are fractional editing amplitudes and k_1 and k_2 are distinct rate constants.

Editing assays in HEK293T cells

HEK293T cells (CRL-11268 ATCC, Manassas, VA) were maintained in Dulbecco's Modified Eagle's Medium supplemented with 10 % (v/v) fetal bovine serum, 1% penicillin–streptomycin solution, 1 mM sodium pyruvate, and 2 mM glutamine. For each transfection, $0.75 - 3 \times 10^5$ cells were seeded in a 35 mm glass-bottom dish and transfected with plasmid DNA two days later. The Effectene® Transfection Reagent kit (QIAGEN, Hilden, Germany) was used according to protocol. All components were co-transfected and the following amounts were used for each transfection: pcDNA 3.1 (−) mCherry-eGFP or mCherry-eGFP W58X (25 ng), pcDNA 3.1 (+) λN-DD, (1–5 λN-DDs and E488Q mutants; 100 ng) and U6 pENTR guide RNA vector (2 μg). For negative controls, the siLacZ U6 RNAi vector that was supplied with the kit was used for transfection in an equal proportion. For controls in the determination of off-target edits, we substituted equal amounts of the following plasmids for the experimental 1boxB and 2boxB RNA guides: pcDNA 3.1(−), pUC18, and siLacZ. Cells were analyzed

24, 48, 72 and 96 h post-transfection for the time-course experiments. For all other experiments cells were analyzed 96 h after transfection.

To determine the extent of eGFP fluorescence correction, cells were imaged with the Cellometer® Vision imaging system (Nexcelom Bioscience, Lawrence, MA, USA) using the dual fluorescence mode. Two monochromatic LED modules were used as the excitation light sources (470 and 525 nm). Each LED was combined with the specific emission filters VB535 and VB595. Raw data were taken from the FCS Express Software (De Novo, Los Angeles, CA, USA) and analyzed in Excel. We selected cells with red fluorescence of over 10,000 counts to ensure minimal background contamination. In order to calculate eGFP correction, we first determined the green to red fluorescence ratio of cells transfected with mCherry-eGFP WT and the precise version and quantity of the editing enzyme and guide RNA used for that experiment. Based on this, we estimated the expected green fluorescence for every mCherry-eGFP W58X cell if correction were at 100 %. Using this number, we could estimate the proportion of correction. Average eGFP fluorescence was measured for 200–800 cells from each experiment, and each experiment was replicated to ensure consistency. One-way ANOVA and the Tukey's test were used for mean comparisons using $P < 0.001$.

To determine editing efficiency based on mRNA correction, total RNA samples were extracted from transfected HEK 293T cells using the RNaqueous kit according to protocol as described before (11). cDNA was synthesized using gene-specific RT-primers and amplified by PCR. The final product was directly sequenced and quantified as described above. Off-target edits were also identified by RT-PCR followed by direct-sequencing. We used 9 % as a threshold for calling an off-target edit. This number was based on the average C/T ratio (antisense sequence) plus one standard deviation for 50 random adenosines in assays that lacked an editing enzyme.

Confocal microscopy

Images were acquired on a specially designed Zeiss Spinning Disk Confocal Imaging System (Zeiss Examiner Z1 Microscope) using a 63X (wet) objective. The same field of cells was excited with either a 488 nm laser for mCherry or a FITC light source for eGFP and emission filter Em01-R488/568 using constant exposure and intensity settings. Cells were imaged in serum free Opti-MEM® (Life technologies, Carlsbad, CA, USA) supplemented with 10 % fetal bovine serum, 20 mM HEPES pH 7.4, 1 mM sodium pyruvate and 2 mM glutamine. Confocal images were used strictly for presentation in the figures. All data analysis was performed on large fields of cells using the Cellometer® Vision as described above.

RESULTS

The goal of this study was to systematically improve a genetically encoded version of our system for SDRE so that it could efficiently and selectively edit a target A in human cells. Our system is multipart (Figure 1A); therefore we focused on multiple components in our efforts to improve it.
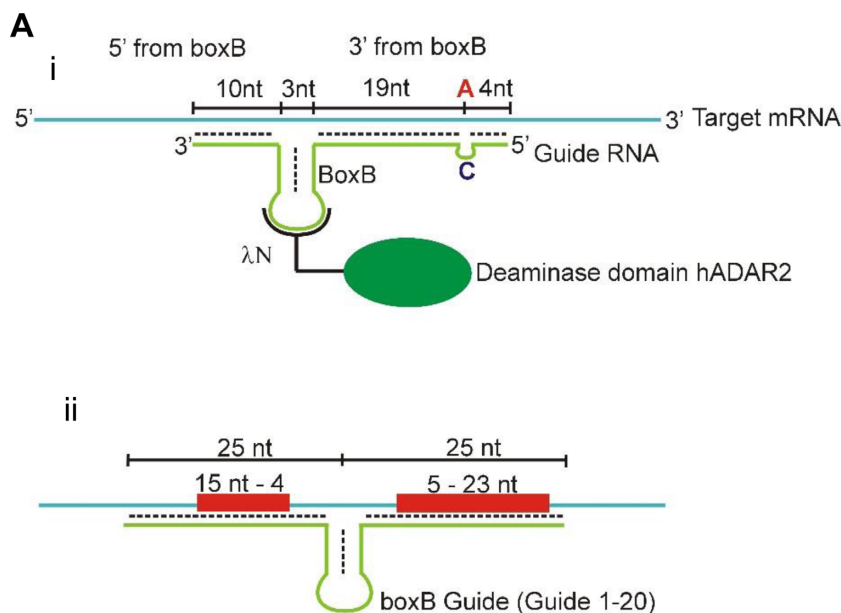
Figure 1. Positions of RNA editing sites relative to boxB in the RNA guide. (**A**i) A schematic of the components in our basic system of SDRE. The target A (shown in red) is located at a position 19 nt on the 3′ side of the boxB hairpin. Our normal guide RNAs contain a C mismatch (shown in blue) with the target A. (**A**ii) Experiments were performed *in vitro* with 20 RNA guides and detailed results of editing at every A is given in Supporting Table S3. Editing hot-spots are highlighted in red, n = 3.

An antisense guide RNA directs the enzymatic reaction to a specific adenosine and also provides a nominally double-stranded structure which is required for deamination (5). The catalytic domain of ADAR performs the editing reaction. The two are linked through an interaction between the λN peptide, attached to the catalytic domain, and a boxB RNA hairpin, attached to the RNA guide. In our previous study (11), a fully genetically encoded version of SDRE edited at a low efficiency in cells. In addition, because of variability, it was difficult to accurately quantify editing efficiency in cells. In the present study, we explored the importance of guide oligo design, the linkage between the λN and the guide, and the catalytic rate of the DD on editing efficiency. We also examined off-target editing within the targeted mRNA, in random endogenous targets and at adenosines known to be edited in humans.

Geometry of guide RNA design

We first focused on the architecture of the guide RNA. At the outset, our basic guide RNA consisted of a boxB loop that was 19 nt on the 5′ side of the target adenosine (to avoid confusion, all references to 5′ and 3′ correspond to the target mRNA and not the RNA guide; see Figure 1Ai). We hypothesized that geometric constraints could limit the access of the deaminase domain to the target A. These constraints could be due to the space occupied by boxB, λN and the catalytic domain, or to constraints imposed by the orientation of these elements when λN is bound to boxB. Accordingly, we decided to test whether the distance between the target A and the boxB loop makes a difference. In addition, we wanted to see if editing could occur on both the 5′ and 3′ side of boxB. To test these questions, we modified our guide design such that the boxB loop was surrounded by a symmetrical 25 nt complementary to the target on either side (Figure 1Aii). Using this architecture, 20 guide RNAs were designed to different regions of a common message, and their ability to drive editing by λN-DD was examined *in vitro* (Supporting Figure S2 and Supporting Tables S3 and S4). Because many guides were tested, we were able to examine editing of A's at every position on both the 5′ and 3′ sides of boxB.

In general, editing efficiency varied between positions. A's close to boxB (3 nt on the 5′ side and 4 nt on the 3′ side), were not edited. However, many examples of efficient editing (>50 %) were observed on both sides of boxB and Figure 1Aii summarizes the results (for a detailed description of experiments see supporting material mentioned above). In general, we found that the well-established neighbor preferences of human ADAR2 (20,21) were more influential than the precise position of the boxB loop. Therefore, manipulating the distance between boxB and the target A appears not to be a useful strategy for improving our system. The observation that efficient editing was observed on either side of the boxB loop was important, however, and this fact led to an improvement in RNA guide design as described in upcoming sections. Moving forward, we decided to continue using our standard guide with the target adenosine 19 nt on the 3′ side of boxB because this position was edited efficiently. We also elected to introduce a cytosine (C) mismatch opposite the target adenosine because this has been shown to increase editing efficiency by others (16,26,27).

A fluorescence reporter system to calibrate the extent of editing in single cells

Because our immediate goal was to improve editing efficiency in transiently transfected human cells, we needed a method to quickly and accurately assess correction. An obvious choice was a fluorescent reporter, containing a PTC,
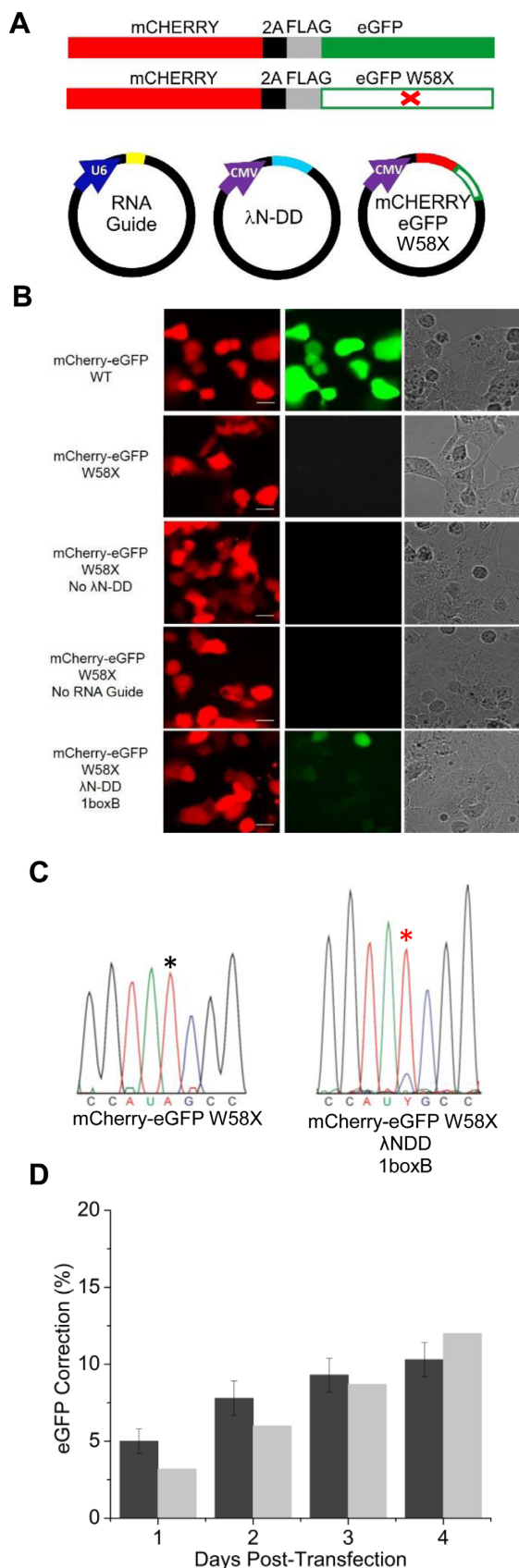
Figure 2. Fluorescent reporter system for quantifying editing. (**A**) Cartoons of fluorescent protein constructs and plasmids used in this study.

which would fluoresce upon correction. In our previous study, we used an eGFP reporter; however, because the efficiency of transient transfections varied, it was difficult to quantitatively assess correction. What we needed was an internal calibration for each cell. Accordingly, we designed a dual fluorescent reporter system (28) consisting of mCherry and eGFP in tandem separated by the self-cleaving 2A peptide and a FLAG epitope-tag (29; Figure 2A). The 2A peptide was added to avoid potential artifacts caused by Fluorescence Resonance Energy Transfer between eGFP and mCherry. Western Blots of HEK 293T cells transiently transfected with this construct showed that 2A peptide cleavage was complete (Supporting Figure S3). When this construct was transfected into HEK 293T cells, we could measure a consistent ratio between red and green fluorescence (first panel Figure 2B). Therefore, the red fluorescence was an accurate predictor of green fluorescence. Next we introduced a PTC (W58X) into eGFP. As expected, cells transfected with this construct showed only red fluorescence (second panel Figure 2B). It should be noted that the adenosine in the W58X PTC (UAG) was in an optimal context for conversion back into the wild-type tryptophan (UGG) by editing. In order to correct W58X, we transfected plasmids encoding mCherry-eGFP W58X and λN-DD, driven by CMV promoters, and a plasmid encoding a guide RNA, driven by a U6 promoter (Figure 2A). The fifth panel in Figure 2B shows restoration of green fluorescence. When either λN-DD or the guide RNA containing plasmids were omitted, no green fluorescence was evident (panels 3 and 4 in Figure 2B). Based on red fluorescence, we estimated that we restored 11% of eGFP fluorescence. Direct sequencing of mCherry-eGFP W58X RT-PCR products from the same reactions gave the same value (11 %; Figure 2C). It should be noted that in all cases described throughout this paper, estimates of correction based on direct sequencing and fluorescence measurements were in close agreement (Supporting Figure S4). Fluorescence measurements and RNA samples were taken 96 h post-transfection. Earlier time points also showed correction, albeit to a lesser extent (Figure 2D). These data confirmed that the dual reporter system could be used to accurately

Full-length mCherry and eGFP were fused together and separated by a 2A peptide (black) followed by a FLAG epitope tag (grey). In addition, a version with a stop codon (UAG) inserted at position 58 of eGFP was made (W58X). These constructs were cloned into a vector driven by the CMV promoter, as was λN-DD. RNA guides were driven by a U6 promoter. (**B**) Confocal images of HEK293T cells transfected with different combinations of components are shown. Red, green, and DIC images are shown for the same field of cells. Pictures are taken 96 h post-transfection. Scale bars = 12 μm. Fluorescence correction was estimated to be 11 ± 0.05 %. (**C**) Sequences from RT-PCR products of corrected cells and cells transfected with mCherry-eGFP W58X alone. Asterisks indicate the target A. Editing percentage for experimental samples was estimated to be 11 %. (**D**) Estimates of editing efficiencies from fluorescence (dark gray) and direct sequencing (light grey) were compared at various days post-transfection. Fluorescence estimates were based on 200–800 cells per sample (mean ± SEM) and RT-PCR products came from the same samples. Technical duplicates for all fluorescence measurements yielded similar results (2.3 ± 0.3, 8.7 ± 1.5, 8.9 ± 1.5, and 12.9 ± 1.4 % for days 1, 2, 3, and 4, respectively). Technical duplicates for RNA correction based on direct sequencing of were as follows: 4, 6, 9 and 14 %, for days 1, 2, 3 and 4, respectively.

assess functional correction by SDRE. They also confirmed that the editing efficiency of our system was low.

Multiple λN peptides improve RNA editing efficiency

To improve SDRE, we focused on the linkage between the deaminase domain and the guide RNA. Our system is two part, and for editing to occur the deaminase domain must bind to the guide via the λN:boxB interaction (11). We reasoned that the affinity of this interaction could be an important determinant of editing efficiency, and that the apparent affinity could be increased by adding more λNs or boxBs. We first looked at the effects of adding more λNs. To test whether this strategy was sound, we added an extra λN to the amino terminus of λN-DD (Figure 3Ai) and purified both the 1λN-DD and 2λN-DD versions from the yeast *Pichia pastoris* (11,22–24). These enzymes were then combined with our standard guide and mCherry-eGFP W58X RNA *in vitro* and reaction kinetics were monitored under single-turnover conditions (Figure 3Aii). The addition of the extra λN increased the reaction rate from 0.1 ± 0.02 to 0.3 ± 0.05 min^{-1}. In addition, it increased the maximum editing percentage from 63.4 ± 2.7 to 90.9 ± 1.1 %. We next tested the effects of extra λNs in cells. Constructs with 1–5 λNs were transfected into HEK293T cells and editing was assessed using our standard assay. Editing efficiency based on fluorescence correction increased from 11 to 35 % with 4λN-DD (Figure 3Aiii). There was no statistically significant improvement between 4λN-DD and 5λN-DD. Direct sequencing, which measured editing at 39 %, was in good agreement with the fluorescent measurements. Thus, increasing the number of protein binding partners increased editing efficiency.

Two boxB hairpins improve RNA editing efficiency further

We next asked whether increasing the number of boxB binding partners would also increase efficiency. Data from Figure 1 demonstrated that λN-DD could edit efficiently on both the 5′ and 3′ sides of boxB. It also showed that a target adenosine 11 nt on the 5′ side was as efficiently edited as one 19 nt on the 3′ side. Based on this, we designed a guide with 2 boxBs, making the target adenosine 11 nt on the 5′ side of one and 19 nt on the 3′ side of the other (Figure 3Bi). We first tested the 2 boxB guides *in vitro* using purified λN-DD under single turnover conditions. The 2 boxB guide visibly increased the reaction rate (Figure 3Bii); however, the reaction kinetics were complex and could not be well fit with a single exponential rate constant. The maximum editing percentage increased from 63 ± 2.7 to 95 ± 0.4 %. We then tested the two boxB guide with enzymes containing 1–4 λNs in HEK293T cells using our reporter assay (Figure 3Biii). The combination of two boxB and four λNs increased the editing percentage to 64 %, as measured by fluorescence, and 57 %, as measured by direct sequencing. Regardless of the number of λNs on the editing enzyme, the additional boxB increased editing (compare Figure 3Aiii and Biii) and the difference was significant in all cases. Thus, increasing the number of RNA or protein binding partners increased editing efficiency. To further improve our strategy, we then looked to modify other elements in our system.

The E488Q mutation in the deaminase domain improves RNA editing efficiency

We next decided to directly manipulate catalysis within the deaminase domain. A previous study showed that a single mutation in a conserved loop near the catalytic center of WT hADAR2 (E488Q), increases the enzyme's catalytic rate (30), and it also increases the affinity, and activity, of the isolated deaminase domain for a substrate RNA (31). We added the E488Q mutation to both λN-DD and 4λN-DD in HEK293T cells (Figure 4A). In both cases, the mutation led to a large increase in editing efficiency. A casual observation of the transfected cells showed that green fluorescence in 4λN-DD E488Q with the 2boxB (Figure 4B) guide was not noticeably different than WT mCherry-eGFP (Figure 2B, panel 1). In these assays, editing efficiency was estimated at 69% by fluorescence and 72 % by RT-PCR (Figure 4C). Thus, the combination of the catalytic mutant with the manipulations of λN and boxB resulted in an increase in editing from ∼11 % to ∼70 %. Nevertheless, as noted before, our reporter system uses an A in an optimal context (UAG) and therefore we would predict that these editing percentages are a best case scenario.

Optimized system for SDRE edits different PTCs

We next explored the ability of our improved SDRE system to edit A's in different neighboring contexts. For these experiments, we focused on A's within PTCs in all possible contexts. To quantify editing, we relied exclusively on RT-PCR (there were not the appropriate tryptophan codons within eGFP to create the constructs to test all permutations via fluorescence). For the UAG and UGAN contexts (codon underlined), correction requires a single deamination. However, for the four UAAN PTCs, two deaminations are required and thus we estimated correction as the product of the fractional conversion for both; however, we also present data for the conversion efficiency of each individual adenosine (Figure 5B). As expected from the nearest neighbor preferences of the deaminase domain (21), the UAG PTC was edited best (Figure 5A). For UGAN PTCs, the identity of the 3′ neighbor is important. UGAG is edited most efficiently by both 4λN-DD and 4λN-DD E488Q. 4λN-DD edits all other 3′ neighbors poorly. 4λN-DD E488Q can edit UGAU and UGAA at high levels but UGAC more poorly. Based on the established nearest neighbor rules, we would have expected UGAC to be edited more efficiently. For UAAN PTCs, the 3′ neighbor of the second adenosine is an important factor for 4λN-DD E488Q where C = A > G = U. For 4λN-DD, all UAAN PTCs are edited poorly. For most contexts, 4λN-DD E488Q edits better than 4λN-DD, but not always. Thus, when targeting new A's it would be prudent to test both.

Off-target RNA editing

Data thus far indicates that A's in a variety of contexts can be targeted efficiently. However, we have not examined whether unintended A's are edited as well. In our previous work, we reported moderate off-target editing in eGFP messages at two positions in transfected HEK293T cells (11). Because our new system edits target A's at a much higher
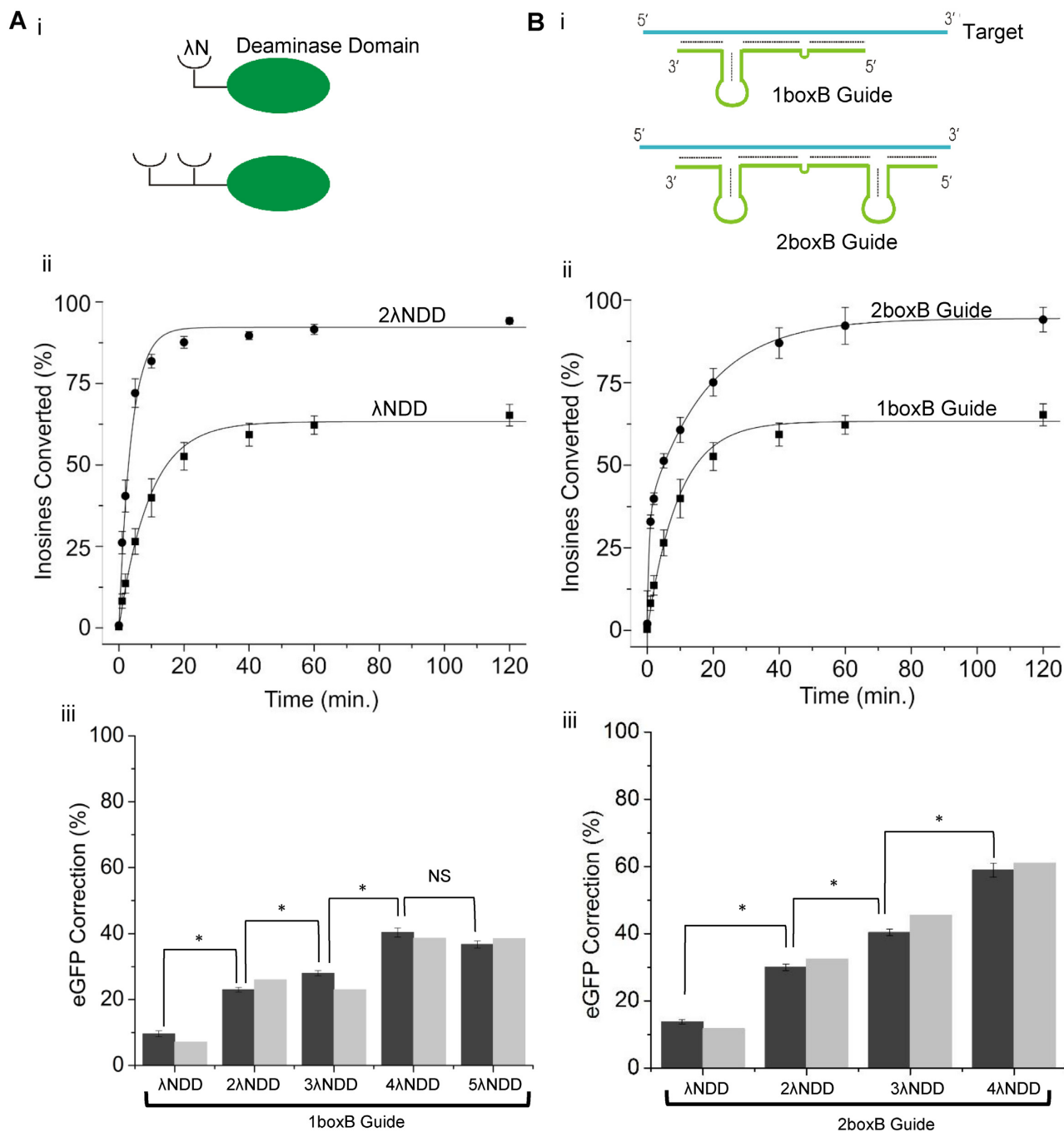
Figure 3. Increasing the number of λNs and boxBs improves editing. (**Ai**) A schematic showing the addition of N-terminal λN's. (**Aii**) Reaction kinetics of λN-DD and 2λN-DD, purified from *Pichia pastoris*, were measured using mCherry-eGFP W58X *in vitro* using our standard 1boxB RNA guide. Rate constants, estimated from fits (see Materials and Methods section), were $k_{obs} = 0.1 \pm 0.02$ and 0.3 ± 0.05 min^{-1} for λN-DD and 2λN-DD, respectively. Experiments were performed at 35°C. Constructs with 1–5λNs connected to DD were generated and tested in HEK293T cells using the fluorescent reporter assay (dark gray) and by RT-PCR (light gray; **Aiii**). Technical duplicates for all fluorescence measurements yielded similar results (11.6 ± 0.5, 19.2 ± 0.9, 32.1 ± 1.3, 38.5 ± 0.7 and 35.7 ± 1.3 % for 1–5λN-DD, respectively). Technical duplicates for RNA correction were as follows: 8, 27, 32, 48 and 41 % for direct sequencing measurements of 1–5λN-DD, respectively. (**Bi**) 1boxB and 2boxB RNA guides. With the 2boxB guide, the target A (red) is 19 nt 3′ to boxB 1 and 11 nt 5′ to boxB 2. (**Bii**) The kinetics of editing using a 1boxB or 2BoxB guide was tested with purified λN-DD and mCherry-eGFP W58X *in vitro*. Temperature = 35°C. The data for 2boxB was fitted to a double exponential and the rate constants were $k_{1\,obs} = 1.54 \pm 0.09$ and $k_{2\,obs} = 0.05 \pm 0.001$. (**Biii**) Editing efficiency of 2boxB guide was tested in HEK293T cells using 1–4λN-DD. As before, correction was estimated by both fluorescence (dark gray) and direct sequencing (light gray). All results were tested with a one-way ANOVA and Tukey's test. An asterisk indicates significance ($P < 0.001$) and NS = not significant. Technical duplicates for all fluorescence measurements yielded similar results (16.9 ± 0.5, 32.9 ± 1.1, 39.4 ± 1.0 and 54.5 ± 1.9 % for 1–4λN-DD, respectively). Technical duplicates for RNA correction were as follows: 13, 30, 48 and 57% for direct sequencing measurements of 1–4λN-DD, respectively. For *in vitro* kinetic measurements (Aii and Bii), $n = 3 \pm$ SEM.

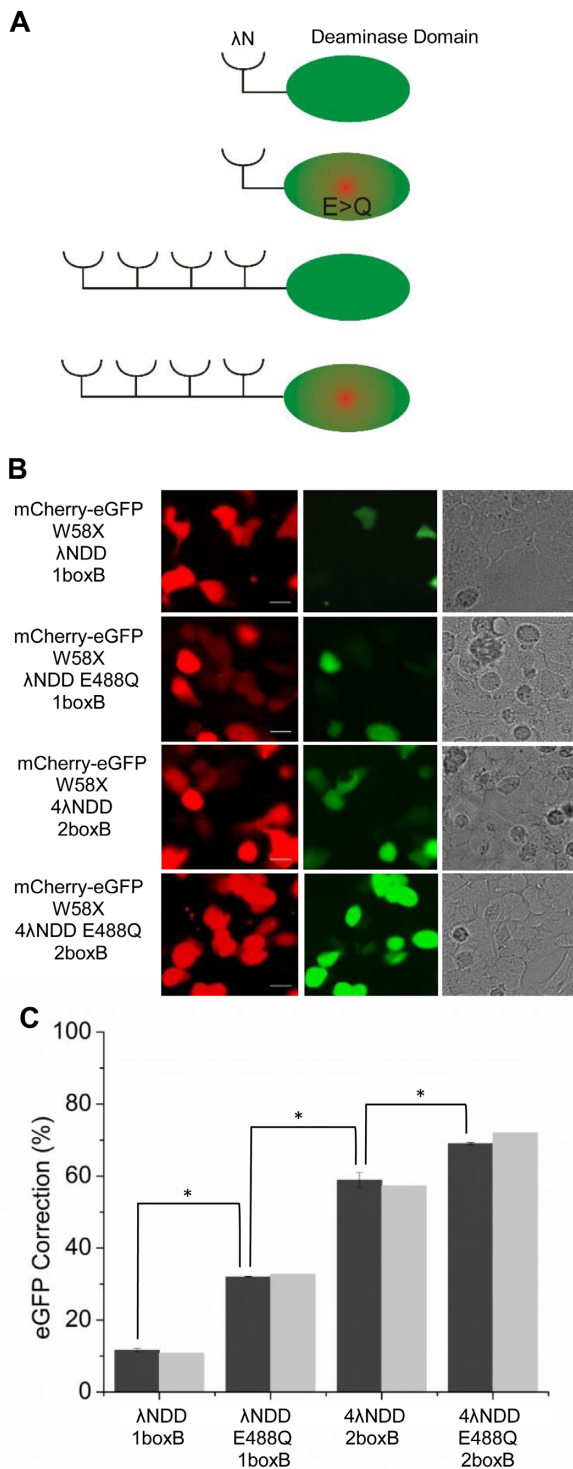**Figure 4.** E488Q mutation introduced into DD increases editing efficiency. (**A**) Schematic of the E488Q mutation in λN-DD or 4λN-DD. (**B**) Confocal images of HEK293T cells transfected with various components of SDRE. Scale bars = 12 μm. (**C**) Quantification of correction in transfections by both fluorescence (dark gray) and direct sequencing (light gray). All values for fluorescence correction are significantly different by ANOVA and Tukey's test. n = 200–800 cells, mean ± SEM. Technical duplicates for all fluorescence measurements yielded similar results (11.5 ± 0.1, 32 ± 0.2, 58.9 ± 2.1 and 65 ± 0.02 for λN-DD 1boxB, λN-DD E488Q 1boxB, 4λN-DD 2boxB and 4λN-DD E488Q 2boxB, respectively). Technical duplicates for RNA correction were as follows: 7, 27, 69 and 70 % for direct sequencing measurements of λN-DD 1boxB, λN-DD E488Q 1boxB, 4λN-DD 2boxB and 4λN-DD E488Q 2boxB, respectively.
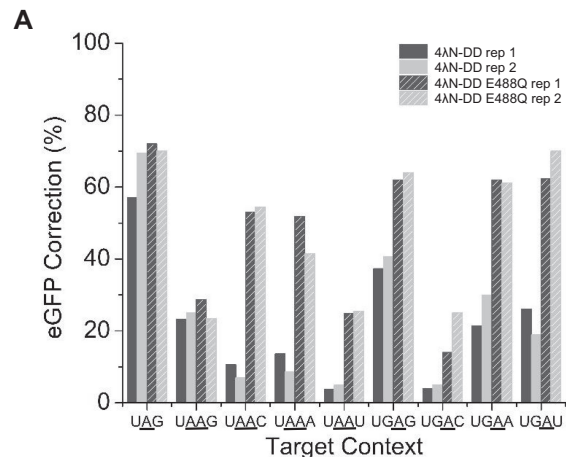

	5'	A		A		3'
		Rep1	Rep2	Rep1	Rep2	
4λN-DD	U	52.8	53.0	47.8	43.7	G
	U	39.8	47.8	17.5	22.3	C
	U	37.1	39.5	23.1	28.0	A
	U	29.8	26.9	16.6	14.1	U
4λN-DD E488Q	U	47.6	52.0	49.3	55.2	G
	U	74.4	78.0	73.1	68.0	C
	U	63.3	74.0	65.6	70.0	A
	U	49.0	50.0	52.0	49.7	U

Figure 5. Editing efficiencies of optimized SDRE system on A's in different neighboring contexts. (**A**) A's in different neighboring contexts were introduced into mCherry-eGFP and different 2boxB guide RNAs were designed to target them. These RNA guides were tested in HEK293T cells with either 4λN -DD or 4λN-DD E488Q. Results were tested only by direct sequencing of RT-PCR products. Experiments were done in duplicate. (**B**) Editing percentages of individual A's for the UAAN context with 4λN -DD and 4λN-DD E488Q. Rep 1 = repetition 1 and rep2 = repetition 2.

efficiency, we decided to revisit the question of off-target editing. Using 4λN-DD, there were 11 off-target edits in mCherry-eGFP transcripts (Supporting Table S1 and Figure 6). Of these, three were in a region complementary to the guide RNA and the rest outside of it. For 4λN-DD E488Q, there were 13 (all 11 of the WT plus 2 additional ones; see Supporting Figure S5). In general, the efficiency of off-target editing is higher with the E488Q mutation. Next, we explored factors that might contribute to off-target editing (Supporting Table S1). For both E488Q and the WT deaminase domain, the number of λN peptides had little influence on off-target edits outside of the region complementary to the RNA guide. Off-target edits complementary to the RNA guide were generally more severe with 4λN peptides than with 1. The number of boxBs in the RNA guide had little effect on off-target editing. Taken together, this data implies that the λN-boxB interaction is not required for off-targets outside of the region complementary to the RNA guide, but it is important for those underneath the guide as well as for the on-target editing site. To test this idea, we mutated λN within λN-DD, 4λN-DD, λN-DD E488Q, and 4λN-DD E488Q at positions known to
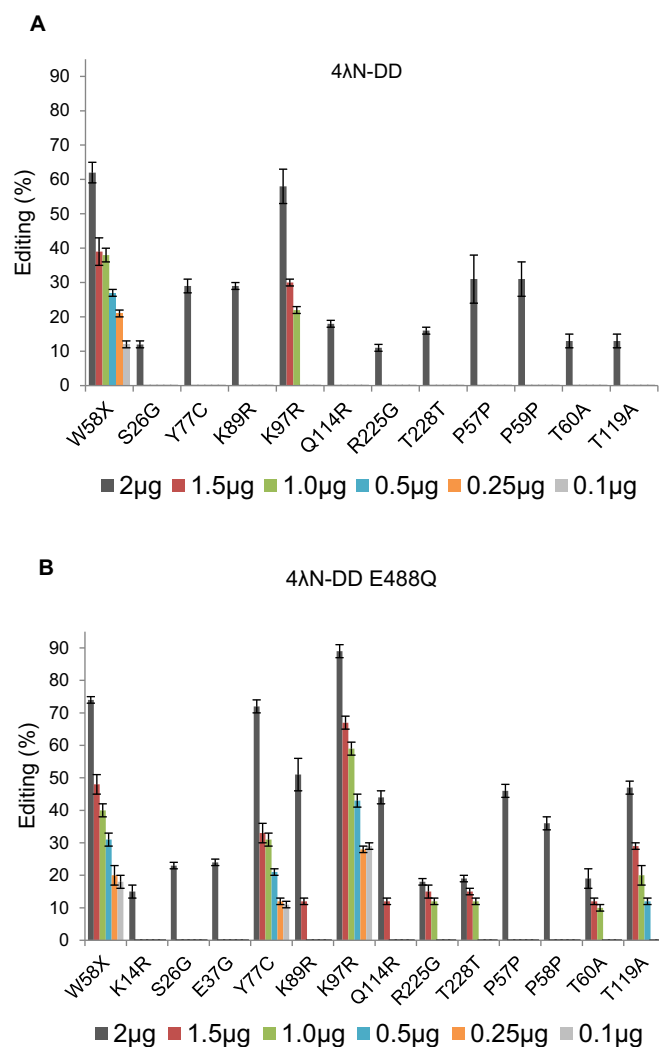
A

B

Figure 6. Off-target edits in mCherry-eGFP RNAs. Relationship between the amount of 2boxB RNA guide plasmid transfected and off-target edits. Codon numbering on the abscissa is for mCherry-eGFP. W58X is the on-target edit. P57P, P59P and T60A are in a region complementary to the RNA guide. Results for 4λN-DD are presented in panel (**A**) and for 4λN-DD E488Q in panel (**B**). All percentages are based on direct sequencing of RT-PCR products. $n = 4$, mean ± SEM.

disrupt the interaction with boxB (R7K, R8K and R11K; 32–34). We also made constructs that lacked the λNs altogether (DD and DD E488Q). In general, these constructs yielded less off-target editing but the effect was not dramatic as most sites persisted. On-target editing however, was drastically reduced in all cases, demonstrating the requirement for the λN-boxB interaction. These results indicate that the overexpression of the deaminase domain alone leads to some off-target editing; however, the relationship appears complex.

We next explored the relationship between the RNA guide and off-target editing (Supporting Table S1). First, we tested whether directing a guide to mCherry-eGFP was required for off-target editing. Here, we used a non-specific 2boxB guide directed against another target (U6 CFTR 2boxB) with 4λN-DD and 4λN-DD E488Q. Surprisingly,

off-target edits were almost identical to those produced with a specific guide. We next tested whether driving a random siRNA (U6 siLacZ) instead of a 2boxB guide would produce the same effect, and it did. However, when we replaced our U6 vector driven guides with generic plasmids (pcDNA 3.1(−) and pUC18), off-target edits were largely abolished with 4λN-DD. For 4λN-DD E488Q, off-target edits were also largely abolished for pcDNA 3.1(−) but only diminished for pUC18. These data indicate that there is a correlation between RNA overexpression and off-target editing and these events are more persistent when using the E488Q mutation. Accordingly, we decided to explore whether we could reduce off-target editing by decreasing the amount of RNA guide transfected (Figure 6). With 4λN-DD, by reducing the amount of guide RNA from 2 to 1.5 μg per transfection, all but one off-target (K97R) was abolished while on-target editing was still robust (∼40 %; reduced from ∼60 %). By using 0.5 μg of RNA guide, all off-targets were abolished, leaving ∼25 % on-target editing. With 4λN-DD E488Q, off-targets are more persistent. Off-target edits were not as sensitive to dilutions of the editing enzyme where both on-target and off-target events decrease more or less concomitantly (Supporting Figure S6). Thus at present, a careful titration of the guide RNA appears to be important for controlling off-target edits.

We also explored whether our system produced off-target edits in mRNAs that were not targeted by our guide. For these experiments we transfected 4λN-DD and 4λN-DD E488Q with 2 μg of 2boxB, conditions that produced robust off-targets in mCherry-eGFP. For these experiments, we amplified and directly sequenced 800–1200 nt portions from five messages expressed in HEK293T cells (hTRPC3, hATP1A1, hATP1B1, hATP1B2 and hEDG3). We did not observe any off-target edits in these sequences. We also looked at four adenosines in three mRNA substrates that are known to be edited in humans (Supporting Table S5; 35–38). For GLI1 nt 2101, we observed no editing in non-transfected HEK293T cells. For cells expressing either editing enzyme, we observed approximately 30% editing that could be reduced to 15% by using 0.5 μg of 2boxB guide RNA. For NEIL1 nt 725, we observed ∼80% editing in WT cells. 4λN-DD had little effect on this site but 4λN-DD E488Q increased editing by ∼10%. For NEIL1 nt 726, we observed ∼35% editing which was about doubled with each editing enzyme at high guide concentrations but unaffected at low concentrations. For AZIN1 nt 1099, we did not detect editing under any condition.

Comparison of catalytic rate of SDRE versus WT ADARs

Relying on a guide RNA instead of dsRBMs, our system for SDRE is fundamentally different than RNA editing by WT ADAR. Although the catalytic rate of WT ADAR varies according to the specific RNA substrate, we wanted to get a general idea of how our system compared. We purified 4λN-DD WT and 4λN-DD E488Q from yeast and measured the catalytic rates on the mCherry-eGFP W58X RNA *in vitro* under single-turnover conditions (Figure 7A). The reactions were too fast to accurately measure at our standard temperature of 35°C, so we reduced the temperature to 15°C. Using a 2boxB guide RNA, the deamination rate
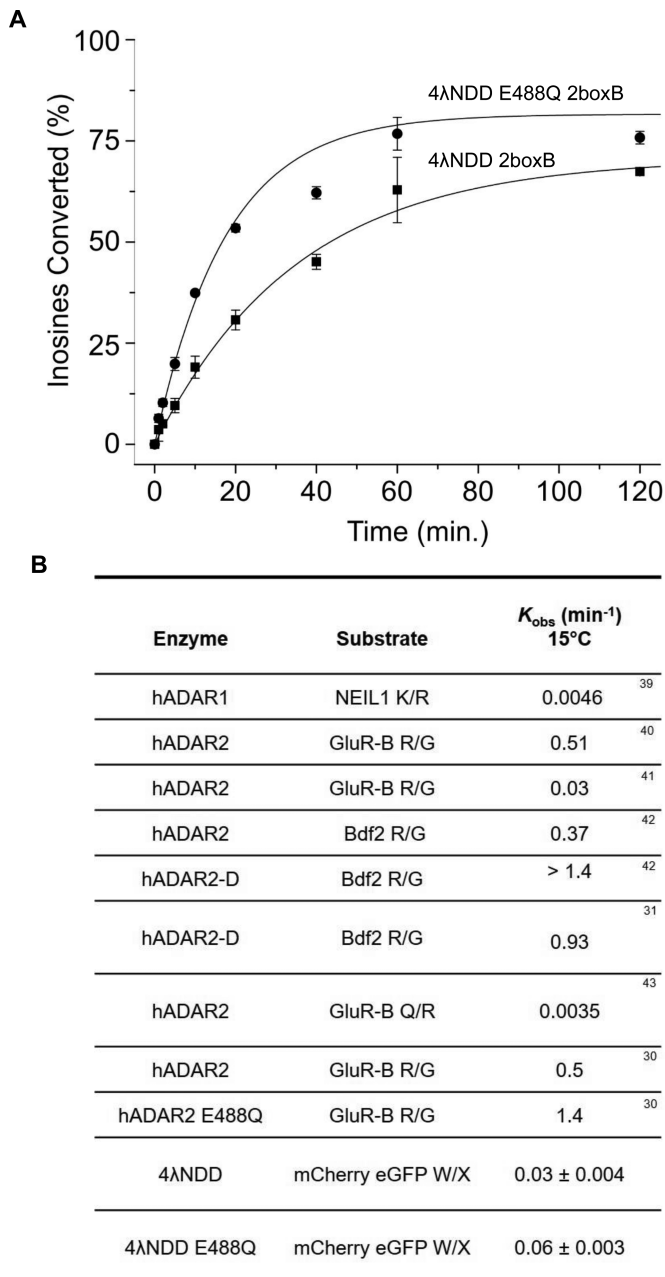
A

B

Enzyme	Substrate	K_{obs} (min^{-1}) 15°C	
hADAR1	NEIL1 K/R	0.0046	[39]
hADAR2	GluR-B R/G	0.51	[40]
hADAR2	GluR-B R/G	0.03	[41]
hADAR2	Bdf2 R/G	0.37	[42]
hADAR2-D	Bdf2 R/G	> 1.4	[42]
hADAR2-D	Bdf2 R/G	0.93	[31]
hADAR2	GluR-B Q/R	0.0035	[43]
hADAR2	GluR-B R/G	0.5	[30]
hADAR2 E488Q	GluR-B R/G	1.4	[30]
4λNDD	mCherry eGFP W/X	0.03 ± 0.004	
4λNDD E488Q	mCherry eGFP W/X	0.06 ± 0.003	

Figure 7. Kinetics of improved system for SDRE compared to reported values for hADARs. (**A**) *In vitro* kinetics of purified 4λN-DD and 4λN-DD E488Q were measured using a 2boxB guide RNA and mCherry-eGFP W58X. Temperature = 15°C. n = 3, mean ± SEM. (**B**) Table of reported values for k_{obs} extrapolated to 15°C using a Q_{10} of 3.2 (see Materials and Methods section). Published values for WT hADAR1, hADAR2, hADAR2 E488Q and hADAR2 DD were measured at either 20°C or 30°C.

for 4λN-DD WT was 0.03 ± 0.004 min^{-1} and for 4λN-DD E488Q was 0.06 ± 0.003 min^{-1}. Published values for WT hADAR1, hADAR2, hADAR2 E488Q and hADAR2 DD were all measured at higher temperatures (20°C and 30°C; 30, 31, 39–43). Accordingly, we estimated the corresponding values at 15°C using a Q_{10} of 3.2 (see Methods Section). The rate constants for both 4λN-DD and 4λN-DD E488Q are about an order of magnitude higher than those for hADAR1 on the NEIL1 K/R site (39) and the hADAR2 GluR-B Q/R site (30; Figure 7B). They are similar to the rate constant given in one report of hADAR2 on the GluR-B R/G site (41). For all other hADAR2 substrates (30,31,40) they are about an order of magnitude slower. For reports on the hADAR2 deaminase domain on the highly editable Bdf2 R/G site (31), and for hADAR2 E488Q on the GluR-B R/G site (30), they are ∼2 orders of magnitude slower. We therefore conclude that our system edits with similar kinetics as WT ADARs on poorer substrates.

DISCUSSION

In this work, we have improved the λN-DD system for SDRE in cells from one that edits a small fraction of the targets A's to one that edits them in the majority of messages, provided that they are in an optimal context. Other contexts are also edited efficiently, but not all. Increases to the apparent affinity between the DD and the guide RNA, and increases to the catalytic efficiency of the DD were the major factors underlying the improvement. Our progress depended on a dual colored fluorescence reporter system that enabled us to calibrate editing within individual cells. Even though improvements have been made, there are still significant limitations that must be overcome to realize the full potential of SDRE.

Although the target A can be converted efficiently, off-target edits occur. In general, there were two classes of off-target edits: those that occurr in sequence complementary to the RNA guide and those that occurr outside of it. The first can presumably be controlled by manipulating the guide sequence (e.g. introducing an A:G mismatch; 11,16,26). The second are more problematic. They could be caused by endogenous, editable structures within the mRNA that are accessible to the docked editing enzyme. In fact, a new method for identifying the targets of RNA binding proteins takes advantage of this activity (44). By attaching the deaminase domain of hADAR2 to RNA binding proteins, their binding partners can be identified by looking for A or G discrepancies in transcriptome sequencing. This highlights the probability that any method that tethers an ADAR deaminase domain to an RNA can lead to off-target events, whether or not an exogenous double-stranded structure is provided with an RNA oligonucleotide. It is also conceivable that off-target edits could be due to the RNA guide binding to unintended places within the mRNA, but we see no evidence of guide complementarity outside of the target. Our data also reveals a complex relationship between RNA overexpression and off-target edits. By carefully titrating the amount of guide RNA used, off-target events can be controlled but at the expense of some on-target editing efficiency. For the mCherry-eGFP message, the use of the E488Q mutation does not appear to be warranted because the modest increase in on-target editing is outweighed by a large increase in off-target editing. Thus, the benefits of this mutation should be determined empirically for each targeted message. We have not yet assessed transcription-wide off-target edits and this is undoubtedly an important step; however, sequencing of a set of random mRNAs revealed no off-target edits outside of the targeted RNA. Editing

of naturally occurring substrates, on the other hand, were modestly affected by SDRE. In general, these data hint at a strategy for reducing off-targets in the future: by increasing the affinity of the editing enzyme for the on-target sites relative to the off-target sites, all components, including the guide RNA, could be delivered in lower amounts.

In addition, manipulations to the guide RNA could conceivably increase the affinity of λN-DD for the target A. At present, the guide RNA has a C mismatch under the target, but the rest is perfectly complementary to its binding partner. Naturally occurring RNA editing substrates do not look like this, having more mismatched positions (6,45–48). The key will be to decide where to put mismatches in the guide RNAs. Molecular modelling or high-throughput screens may help solve this problem. The introduction of mismatches to guide RNAs may also improve editing of A's in poor neighboring contexts. Another strategy for improving SDRE is to use DDs from different ADARs (16), or to select for further mutants within the DD of hADAR2. In our system, we have elected to use the deaminase domain from hADAR2 because this enzyme is known to underlie most recoding events in humans. However, it is likely that adenosines which lie in specific contexts might be best converted using a different catalytic domain or at least by introducing targeted mutations. The recent structure of the catalytic domain of hADAR2 bound to an RNA substrate will be a tremendous benefit in these efforts (49). Finally, editing using our system presumably takes place in the cytoplasm because the nuclear localization signal of hADAR2 resides at the amino-terminus, a region we have removed (50). This stands in contrast with endogenous RNA editing which takes place in the nucleus at the level of pre-mRNA (6,46,51). Perhaps driving editing within the nucleus could reduce off-target events. A better optimized system for SDRE would be useful for biological research or therapeutic applications.

A major difference between SDRE and genome editing is that the first is transient and the second permanent. It should be noted that most therapeutics are transient as well, so targeting genetic information within RNA has advantages in some cases. Even for hereditary diseases, where a permanent correction would be desirable, SDRE has advantages: off-target changes are not as dangerous in a transient system and RNA is more accessible than DNA. A significant disadvantage with SDRE at present is the fact that it is limited to A to I changes; however, other RNA modification systems exist, the most notable being the cytosine deaminases which convert cytosine to uracil (52). For future applications SDRE holds much promise. Not only can it be used to correct genetic defects but also to fine-tune protein function.

SUPPLEMENTARY DATA

Supplementary Data are available at NAR Online.

ACKNOWLEDGEMENTS

FUNDING

REFERENCES

1. Napoli,C., Lemieux,C. and Jorgensen,R. (1990) Introduction of a chimeric chalcone synthase gene into petunia results in reversible co-suppression of homologous genes in trans. *Plant Cell*, **2**, 279–289.
2. Fire,A., Xu,S., Montgomery,M.K., Kostas,S.A., Driver,S.E. and Mello,C.C. (1998) Potent and specific genetic interference by double-stranded RNA in Caenorhabditis elegans. *Nature*, **391**, 806–811.
3. Jinek,M., Chylinski,K., Fonfara,I., Hauer,M., Doudna,J.A. and Charpentier,E. (2012) A programmable dual-RNA – guided DNA endonuclease in adaptive bacterial immunity. *Science*, **337**, 816–822.
4. Bass,B.L. and Weintraub,H. (1987) A developmentally regulated activity that unwinds RNA duplexes. *Cell*, **48**, 607–613.
5. Bass,B.L. and Weintraub,H. (1988) An unwinding activity that covalently modifies its double-stranded RNA substrate. *Cell*, **55**, 1089–1098.
6. Melcher,T., Maas,S., Herb,A., Sprengel,R., Seeburg,P.H. and Higuchi,M. (1996) A mammalian RNA editing enzyme. *Nature*, **379**, 460–464.
7. O'Connell,M.A., Gerber,A. and Keegan,L.P. (1998) Purification of native and recombinant double-stranded RNA-specific adenosine deaminases. *Methods*, **15**, 51–62.
8. Kim,U., Wang,Y., Sanford,T., Zeng,Y. and Nishikura,K. (1994) Molecular cloning of cDNA for double-stranded RNA adenosine deaminase, a candidate enzyme for nuclear RNA editing. *Proc. Natl. Acad. Sci. U. S. A.*, **91**, 11457–11461.
9. Basilio,C., Wahba,A.J., Lengyel,P. and Speyer,J.F. (1962) Synthetic polynucleotides and the amino acid code, V*. *Biochemistry*, **48**, 613–616.
10. Macbeth,M.R., Schubert,H.L., Vandemark,A.P., Lingam,A.T., Hill,C.P. and Bass,B.L. (2005) Inositol hexakisphosphate is bound in the ADAR2 core and required for RNA editing. *Science*, **309**, 1534–1539.
11. Montiel-Gonzalez,M.F., Vallecillo-Viejo,I., Yudowski,G.A. and Rosenthal,J.J.C. (2013) Correction of mutations within the cystic fibrosis transmembrane conductance regulator by site-directed RNA editing. *Proc. Natl. Acad. Sci. U.S.A.*, **110**, 18285–18290.
12. Vogel,P., Schneider,M.F., Wettengel,J. and Stafforst,T. (2014) Improving site-directed RNA editing in vitro and in cell culture by chemical modification of the guideRNA. *Angew. Chem. Int. Ed. Engl.*, **53**, 6267–6271.
13. Stafforst,T. and Schneider,M.F. (2012) An RNA-deaminase conjugate selectively repairs point mutations. *Angew. Chem. Int. Ed. Engl.*, **51**, 11166–11169.
14. Vogel,P. and Stafforst,T. (2014) Site-directed RNA editing with antagomir deaminases: a tool to study protein and RNA function. *ChemMedChem*, **9**, 2021–2025.
15. Hanswillemenke,A., Kuzdere,T., Vogel,P., Jekely,G. and Stafforst,T. (2015) Site-directed RNA editing in vivo can be triggered by the light-driven assembly of an artificial riboprotein. *J. Am. Chem. Soc.*, doi:10.1021/jacs.5b10216.

16. Schneider,M.F., Wettengel,J., Hoffmann,P.C. and Stafforst,T. (2014) Optimal guideRNAs for re-directing deaminase activity of hADAR1 and hADAR2 in trans. *Nucleic Acids Res.*, **42**, 1–9.

17. Austin,R.J., Xia,T., Ren,J., Takahashi,T.T. and Roberts,R.W. (2002) Designed arginine-rich RNA-binding peptides with picomolar affinity. *J. Am. Chem. Soc.*, **124**, 10966–10967.

18. Keryer-Bibens,C., Barreau,C. and Osborne,H.B. (2008) Tethering of proteins to RNAs by bacteriophage proteins. *Biol. Cell*, **100**, 125–138.

19. Baron-Benhamou,J., Gehring,N.H., Kulozik,A.E. and Hentze,M.W. (2004) Using the lambdaN peptide to tether proteins to RNAs. *Methods Mol. Biol.*, **257**, 135–154.

20. Lehmann,K.A. and Bass,B.L. (2000) Double-stranded RNA adenosine deaminases ADAR1 and ADAR2 have overlapping specificities. *Biochemistry*, **39**, 12875–12884.

21. Eggington,J.M., Greene,T. and Bass,B.L. (2011) Predicting sites of ADAR editing in double-stranded RNA. *Nat. Commun.*, **2**, 319.

22. Palavicini,J.P., Connell,M.A.O. and Rosenthal,J.J.C. (2009) An extra double-stranded RNA binding domain confers high activity to a squid RNA editing enzyme. *RNA*, **15**, 1208–1218.

23. Keegan,L.P., Rosenthal,J.J., Roberson,L.M. and O'Connell,M.A. (2007) Purification and assay of ADAR activity. *Methods Enzymol.*, **424**, 301–317.

24. Ring,G.M., O'Connell,M.A. and Keegan,L.P. (2004) Purification and assay of recombinant ADAR proteins expressed in the yeast Pichia pastoris or in Escherichia coli. *Methods Mol. Biol.*, **265**, 219–238.

25. Rinkevich,F.D., Schweitzer,P.A. and Scott,J.G. (2012) Antisense sequencing improves the accuracy and precision of A-to-I editing measurements using the peak height ratio method. *BMC Res. Notes*, **5**, 63.

26. Wong,S.K., Sato,S. and Lazinski,D.W. (2001) Substrate recognition by ADAR1 and ADAR2. *RNA*, **7**, 846–858.

27. Källman,A.M., Sahlin,M. and Öhman,M. (2003) ADAR2 A→I editing: Site selectivity and editing efficiency are separate events. *Nucleic Acids Res.*, **31**, 4874–4881.

28. Dolnikov,A., Shen,S., Millington,M., Passioura,T., Pedler,M., Rasko,J.E.J. and Symonds,G. (2003) A sensitive dual-fluorescence reporter system enables positive selection of ras suppressors by suppression of ras-induced apoptosis. *Cancer Gene Ther.*, **10**, 745–754.

29. Ryan,M.D., King,A.M.Q. and Thomas,G.P. (1991) Cleavage of foot-and-mouth disease virus polyprotein is mediated by residues located within a 19 amino acid sequence. *J. Gen. Virol.*, **72**, 2727–2732.

30. Kuttan,A. and Bass,B.L. (2012) Mechanistic insights into editing-site specificity of ADARs. *Proc. Natl. Acad. Sci. U.S.A.*, **109**, E3295–E3304.

31. Phelps,K.J., Tran,K., Eifler,T., Erickson,A.I., Fisher,A.J. and Beal,P.A. (2015) Recognition of duplex RNA by the deaminase domain of the RNA editing enzyme ADAR2. *Nucleic Acids Res.*, **43**, 1123–1132.

32. Su,L., Radek,J.T., Hallenga,K., Hermanto,P., Chan,G., Labeots,L.A. and Weiss,M.A. (1997) RNA recognition by a bent alpha-helix regulates transcriptional antitermination in phage lambda. *Biochemistry*, **36**, 12722–12732.

33. Cilley,C.D. and Williamson,J.R. (1997) Analysis of bacteriophage N protein and peptide binding to boxB RNA using polyacrylamide gel coelectrophoresis (PACE). *RNA*, **3**, 57–67.

34. Legault,P., Li,J., Mogridge,J., Kay,L.E. and Greenblatt,J. (1998) NMR structure of the bacteriophage lambda N peptide/boxB RNA complex: recognition of a GNRA fold by an arginine-rich motif. *Cell*, **93**, 289–299.

35. Li,J.B., Levanon,E.Y., Yoon,J.-K., Aach,J., Xie,B., Leproust,E., Zhang,K., Gao,Y. and Church,G.M. (2009) Genome-wide identification of human RNA editing sites by parallel DNA capturing and sequencing. *Science*, **324**, 1210–1213.

36. Chen,L., Li,Y., Lin,C.H., Chan,T.H.M., Chow,R.K.K., Song,Y., Liu,M., Yuan,Y.-F., Fu,L., Kong,K.L. *et al.* (2013) Recoding RNA editing of AZIN1 predisposes to hepatocellular carcinoma. *Nat. Med.*, **19**, 209–216.

37. Yeo,J., Goodman,R.a, Schirle,N.T., David,S.S. and Beal,P.A. (2010) RNA editing changes the lesion specificity for the DNA repair enzyme NEIL1. *Proc. Natl. Acad. Sci. U.S.A.*, **107**, 20715–20719.

38. Shimokawa,T., Rahman,M.F.-U., Tostar,U., Sonkoly,E., Ståhle,M., Pivarcsi,A., Palaniswamy,R. and Zaphiropoulos,P.G. (2013) RNA editing of the GLI1 transcription factor modulates the output of Hedgehog signaling. *RNA Biol.*, **10**, 321–333.

39. Mizrahi,R.A., Phelps,K.J., Ching,A.Y. and Beal,P.A. (2012) Nucleoside analog studies indicate mechanistic differences between RNA-editing adenosine deaminases. *Nucleic Acids Res.*, **40**, 9825–9835.

40. Macbeth,M.R., Lingam,A.T. and Bass,B.L. (2004) Evidence for auto-inhibition by the N terminus of hADAR2 and activation by dsRNA binding. *RNA*, **10**, 1563–1571.

41. Yi-Brunozzi,H.Y., Easterwood,L.M., Kamilar,G.M. and Beal,P.A. (1999) Synthetic substrate analogs for the RNA-editing adenosine deaminase ADAR-2. *Nucleic Acids Res.*, **27**, 2912–2917.

42. Eifler,T., Pokharel,S. and Beal,P.A. (2013) RNA-Seq analysis identifies a novel set of editing substrates for human ADAR2 present in Saccharomyces cerevisiae. *Biochemistry*, **52**, 7857–7869.

43. Stephens,O.M., Haudenschild,B.L. and Beal,P.A. (2004) The binding selectivity of ADAR2's dsRBMs contributes to RNA-editing selectivity. *Chem. Biol.*, **11**, 1239–1250.

44. McMahon,A.C., Rahman,R., Jin,H., Shen,J.L., Fieldsend,A., Luo,W. and Rosbash,M. (2016) TRIBE: hijacking an RNA-editing enzyme to identify cell-specific targets of RNA-binding proteins. *Cell*, **165**, 742–753.

45. Higuchi,M., Single,F.N., Köhler,M., Sommer,B., Sprengel,R. and Seeburg,P.H. (1993) RNA editing of AMPA receptor subunit GluR-B: a base-paired intron-exon structure determines position and efficiency. *Cell*, **75**, 1361–1370.

46. Lomeli,H., Mosbacher,J., Melcher,T., Höger,T., Geiger,J.R., Kuner,T., Monyer,H., Higuchi,M., Bach,a and Seeburg,P.H. (1994) Control of kinetic properties of AMPA receptor channels by nuclear RNA editing. *Science*, **266**, 1709–1713.

47. Yang,J.H., Sklar,P., Axel,R. and Maniatis,T. (1997) Purification and characterization of a human RNA adenosine deaminase for glutamate receptor B pre-mRNA editing. *Proc. Natl. Acad. Sci. U.S.A.*, **94**, 4354–4359.

48. Maas,S., Melcher,T., Herb,A., Seeburg,P.H., Keller,W., Krause,S., Higuchi,M. and O'Connell,M.A. (1996) Structural requirements for RNA editing in glutamate receptor pre-mRNAs by recombinant double-stranded RNA adenosine deaminase. *J. Biol. Chem.*, **271**, 12221–12226.

49. Matthews,M.M., Thomas,J.M., Zheng,Y., Tran,K., Phelps,K.J., Scott,A.I., Havel,J., Fisher,A.J. and Beal,P.A. (2016) Structures of human ADAR2 bound to dsRNA reveal base-flipping mechanism and basis for site selectivity. *Nat. Struct. Mol. Biol.*

50. Desterro,J.M.P., Keegan,L.P., Lafarga,M., Berciano,M.T., O'Connell,M. and Carmo-Fonseca,M. (2003) Dynamic association of RNA-editing enzymes with the nucleolus. *J. Cell Sci.*, **116**, 1805–1818.

51. Sansam,C.L., Wells,K.S. and Emeson,R.B. (2003) Modulation of RNA editing by functional nucleolar sequestration of ADAR2. *Proc. Natl. Acad. Sci. U.S.A.*, **100**, 14018–14023.

52. Betts,L., Xiang,S., Short,S.a, Wolfenden,R. and Carter,C.W. (1994) Cytidine deaminase. The 2.3 A crystal structure of an enzyme: transition-state analog complex. *J. Mol. Biol.*, **235**, 635–656.